Applied Energy 294 (2021) 116988

Contents lists available at ScienceDirect

Applied Energy

journal homepage: www.elsevier.com/locate/apenergy

Balancing services by run-of-river-hydropower at low reservoir amplitudes: Potentials, revenues and emission impacts

Bastian Hase *, Christian Seidel

Arbeitsgruppe Regenerative Energien, Institut für Statik, Technische Universität Braunschweig, Braunschweig, Germany

HIGHLIGHTS

- Low reservoir amplitudes in run-of-river hydropower enable extensive grid balancing.
- 1 MW of hydropower can facilitate grid integration of up to 11.6 MW of wind or PV.
- Potentials for negative balancing services significantly higher than for positive.
- Providing balancing services reduces overall energy production.
- Nevertheless balancing services can increase the total incomes.

ARTICLE INFO

Keywords:
Run-of-river hydropower
Short-term storage
Control power
Balancing services
Germany

ABSTRACT

The increasing shares of wind energy and photovoltaics in many countries challenge the energy systems in a twofold way. On one hand, there is an increased need for balancing energy in order to compensate abrupt changes in load or power generation. On the other hand, fossil plants being important providers of balancing services are gradually driven out of the system creating a need for renewable substitutes. Due to strict requirements on the upstream water level regime German run-of-river (ROR)-hydropower has until now remained largely unused for providing positive balancing services. However, in this paper we present a novel optimized operation scheme allowing ROR-plants to exactly keep their production schedule and, in addition to that, provide positive and negative balancing services even under these constraints. Our simulations on an exemplary power plant with a very low head show that huge unused balancing power potentials can be expected for ROR-hydropower in Germany enabling a multiplication of fluctuating renewable energy sources. Next to these potentials under current market conditions, this paper elaborates the economic and ecologic aspects of balancing operation.

1. Introduction

In order to reduce the greenhouse gas emissions of the electricity sector the German government has set ambitious goals, aiming for a share of 65% renewables by 2030 [1] and a phase out of coal by 2038 [2]. Due to the national potentials of renewable energies, this will require a huge increase of installed wind [3] and photovoltaic (PV) power [4–6]. This requirement is even increased by the ongoing nuclear phase out [7] and the intended electrification of major parts of the transport and heating sector [1].

The situation in Germany is only an example for the challenges many countries will face in order to comply with the agreements of the COP21 in Paris to limit the global warming to 1.5–2 °C compared to preindustrial level [8]. Therefore, the findings of this paper similarly apply to almost any country that has to replace high current shares of fossil or nuclear power generation by mainly fluctuating renewables.

Their unsteady production hampering exact forecasts is the major challenge for the integration of wind power and photovoltaics into the energy system. Maintaining the equilibrium between load and power production at all times is essential for the functionality of the electric supply system. It is therefore one of the key tasks for electric grid operators. Whenever this balance is disturbed, transmission system operators (TSOs) have to activate positive or negative balancing power in order to temporarily increase or decrease the total power fed into or

* Corresponding author.
E-mail address: b.hase@tu-bs.de (B. Hase).

https://doi.org/10.1016/j.apenergy.2021.116988
Received 23 December 2020; Received in revised form 14 April 2021; Accepted 19 April 2021
Available online 3 May 2021
0306-2619/© 2021 Elsevier Ltd. All rights reserved.

taken from the grids. Using a probabilistic-analytical approach, Hirth et al. concluded that each Gigawatt of additional wind or PV power increases the required amount of balancing energy by 30–70 MW, depending on the improvements achieved in the forecasting accuracy [9]. Even though the authors stress that fluctuating renewables are only of several influencing factors, an increased demand for balancing services can be expected for the next decades [10–12].

In the 'ENTSO-E Regional Group Continental Europe', which includes 24 countries, balancing services are traded as three main products [13,14]. Frequency containment reserve (FCR) - the fastest among them - has to be fully active in 30 s. It is procured by the TSOs in symmetric positive and negative power bands on a capacity base. The automatic frequency restoration reserve (aFRR) has an activation time of 5 min while this period is 15 min for the manual frequency restoration reserve (mFRR). Unlike FCR, both types of positive and negative frequency restoration reserve are traded independently. Moreover, providers receive separate remuneration for reserved capacities (power price) and the balancing energy actually delivered (energy price). Together, these balancing services and a market-price oriented intermittent power production are commonly referred to as 'flexibility' [15].

Due to their ability to store water in reservoirs, both, (pumped-) storage power plants and cascades of ROR-hydropower in so called 'hydropeaking operation' [16] are well suited to provide flexibility to the system [15,17]. 'Peaking' cascades include a large head reservoir and usually one or more downstream buffers, allowing a wide variation of water flow and electricity production within a short period of time. Next to serving as long term storages (pumped-) storages and 'hydropeaking' ROR [18] also have become important providers of balancing services [19]. Especially for grid balancing by (pumped-) storage hydropower numerous investigations have been conducted [20–22]. 'Hydropeaking' of ROR-cascades, however, is increasingly disputed as high amplitudes and gradients in flow rates and water levels, coming along with it, can cause significant stress on the river ecology and morphology [23–27].

The vast majority of German ROR-hydropower is under conventional (i.e. non 'hydropeaking') operation with quasi-steady upstream water levels allowing only small amplitudes [28,29]. Consequently, their power production is largely determined by the flow rate of the river. To date, conventional ROR-hydropower is only known to participate in negative balancing markets [19,30]. In this case the plant remains to be operated at constant upstream water levels and excess water resulting from power reduction is spilled over the weirs.

For both, the production of positive and negative balancing services together or for reducing the water losses over the weirs, a flexible upstream regime is necessary. When maintained within a limited band this is technically feasible for most conventional ROR-plants [31] and can be even ecologically desirable [32]. Recent studies showed the technical feasibility of a peak-to-peak amplitude of 30 cm [31] and above [33] for most rivers in Germany, including those used as waterways. This amplitude is about the same size as waves caused by cargo ships and well below the highest waves occurring on inland waterways [34]. Where this degree of variation is impeded by minimum depths or vertical clearances, a run-through-storage operation, using the reservoir of an upper hydroelectric plant as a common storage, can be implemented [31].

Although research on this topic is scarce [22], several authors proposed to use storage capacities of conventional ROR in order to provide flexibility and balancing services: Rothstein et al. developed criteria for the feasibility of a low amplitude run-through-storage on cascades on the river Neckar and assess average storage times [35]. Seidel [31,36] and Mayer at al. [33] calculated the cumulated energy storage capacity that could be realized by German ROR under exploitation of the tolerable amplitudes in the upstream.

However, these works did not quantify the balancing potentials resulting from a use of these short term storage. Conrad et al. simulated the flexibility potentials of eight conventional ROR-hydropower plants at an hourly resolution, using a deterministic model with perfect foresight [37]. In our paper we simulate the participation of an exemplary conventional ROR-hydropower plant in the markets for FCR, aFRR and mFRR. Next to providing balancing services the storage capacity is used to produce the remaining 'base-power' exactly as scheduled one hour before the start of delivery. With a feasible delivery time of 3 h these schedules can help reducing marketing risks for plant owners and facilitates the forecasting of load grid capacities.

Unlike previous research our model includes prediction uncertainties of the inflow to the reservoir and the activation of balancing power, plant owners are facing. The deterministic simulations use historic 15-minute input values for reservoir inflow and balancing energy activation of the years 2015–2017. The internal resolution is variable with a maximum step size of one minute. Next to giving an overview of the huge potentials that can be expected from ROR-hydropower, this paper illustrates the economic perspectives coming along with balancing operation. Beforehand we give a brief overview about the status quo and possible future trends in the German balancing markets. Legal requirements that can be an obstacle for a flexible operation will not be considered in this paper.

Precursory results achieved with our simulation model are accessible in [38]. This conference paper includes an analysis of feasible lead times and delivery times for base power marketing and an investigation on the optimal lead water level. The presented potentials for FCR and aFRR, however, were calculated for an anterior auction design and therefore deviate from the updated potentials in this paper.

2. A lack of balancing capacities?

Prior to participation in the balancing markets every unit has to prove its technical feasibility in a prequalification process. Generally speaking, balancing capacities can be provided by power production facilities, energy consumers (i.e. demand side management) and by storages, being able to act as producers and consumers. Fig. 1 shows the prequalified power capacities for the standardized balancing products as of September 2020 in Germany [39]. The pool of prequalified units shows high shares of fossil and nuclear technologies, ranging between 25.5% for negative aFRR and 53.4% for positive mFRR. When only considering the phase out of nuclear and coal based power generation, between 12.1% (neg. aFRR) and 28.0% (neg. mFRR) of the current capacities will be lost by 2038.

Hydropower has, by far, the highest prequalified capacities for all

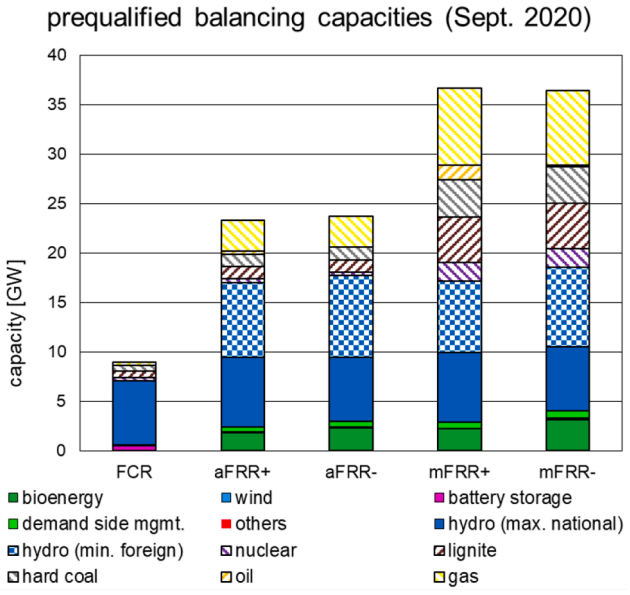


Fig. 1. Prequalified balancing capacities as of September 2020 by technology.

types of balancing services. According to own investigations, currently operating pumped storage capacities in Germany sum up to a turbine power of 6404 MW and a pumping power of 5991 MW. The pure storage hydro power capacity amounts to 371 MW. In addition to that, 690 MW of ROR-hydropower are likely to be in 'hydropeaking' operation. Consequently, German hydropower can at maximum account for 7514 MW of positive balancing services, which is approximately half of the prequalified hydropower capacities for either, positive automatic or manual frequency restoration reserve. As there is a common market for balancing services between Germany and Austria the remaining capacities can most likely be related to Germany's alpine neighbor.

The brown columns in Fig. 2 show the maximum capacities auctioned between January and September of 2020 for the different balancing services. When comparing these figures with the prequalified capacities in Fig. 1 the theoretical offer is at least one magnitude higher than the demand.

This picture changes, however, when looking at the secured supply in a future scenario with neither fossil nor nuclear power generation. In this case, the complete demand for balancing services has to be covered by renewable technologies, battery storage, demand side management and other sources. The remaining prequalified capacities actually available for covering the demand for balancing services are furthermore limited by two factors. Firstly, each unit can only deliver one type of balancing service at the same time, no matter if it is prequalified for several types or not. Secondly, the TransmissionCode 2007 demands TSOs to allocate at least 2/3 of their demand for balancing services within their balancing zone [40]. Even though this share does not apply to the actual activation of balancing energy, the amount of balancing power that can be imported from neighboring balancing zones can eventually even become zero due to limited grid capacities [41]. Depending on future progress in grid reinforcements and interconnectors this could impede massive imports of hydro-generated balancing services from alpine countries. For a conservative scenario with complete redundancy these import capacities should therefore be neglected. Those two limitations severely reduce the hydro power capacities available for balancing services. In Fig. 2, the total national hydropower capacities without conventional ROR, theoretically available for balancing, are shown as blue bars. For the calculations it was assumed that the sum of hydropower plants constantly runs at their average annual production power. These are 22.3% of the rated power

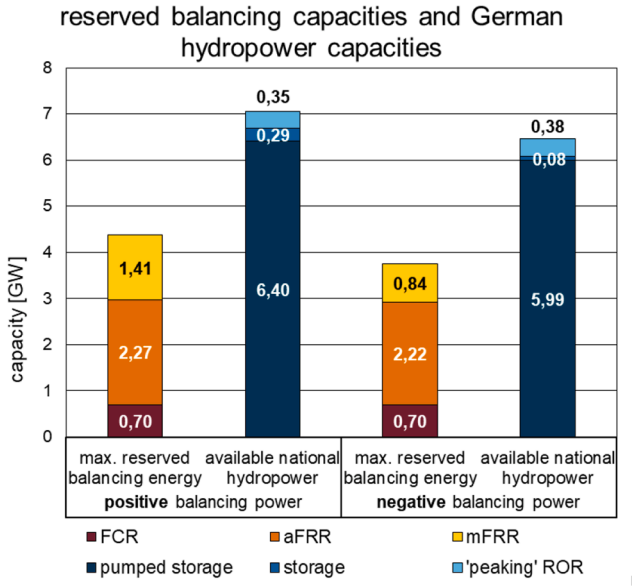


Fig. 2. Comparison of the maximum reserved balancing capacities (Jan.-Sept. 2020) with the hydropower technologies formerly proven to provide balancing services.

for hydro-storage and 52.1% for 'hydropeaking' ROR (as extrapolated from data of the cascade on the river Lech [16]). When using their entire power reserves as balancing capacity, these hydropower technologies could theoretically cover the current demand for positive balancing power by 1.6-times and around 1.5-times of the demand for negative balancing power, respectively, both numbers including FCR.

However, these capacities can hardly be used completely for grid balancing, due to two main reasons. Firstly, the power production of hydropower plants can strongly be affected by seasonal changes, depending on their storage capacities [20,42]. Even for plants connected to storages with sufficient capacities to buffer the seasonal variations of their natural inflow an intermittent water discharge and power production can be necessary for non-energetic reasons [16]. These can be additional demands for water management such as flood prevention or the stabilization of water levels in subordinate rivers [43]. Secondly, (pumped-) storages and 'hydropeaking' ROR-cascades can commonly serve as daily, weekly or even yearly storages at high efficiencies [44]. In a future energy system this ability will be required for backing up wind power and PV during nights, calm winds or peak demands. However, any power band reserved for providing long term flexibility is lost for simultaneous balancing. As a result, their required role as a long term storage significantly decreases the secured balancing reserves of both, (pumped-) storage and 'peaking' ROR-hydropower.

Meanwhile, the multiplication of installed wind power and PV will also increase the need for balancing services [10,11]. As a result, additional capacities or technologies will be needed to ensure the functionality of the balancing markets and prevent scarcity events.

3. Methods and simulation strategy

This section describes the model set up for simulating the simultaneous supply of constant base power and each one of the three balancing services i.e. FCR, aFRR and mFRR. The balancing energy potentials of a ROR-plant are mainly defined by the hydrological circumstances of the site and to a lower extend by the hydro-technology used. In order to keep the influence of the applied technology as low as possible, the plant's inertia was neglected in the simulations. However, the dynamics of common ROR-technologies are well researched [22,45–47] and can be implemented into the model at a later stage. In the investigated combined operation mode, the total power production is the sum of the base power $P_{B,i}$, that is held constant during the length of each marketing interval i, and the balancing power $P_C(t)$ activated by the TSO. As the total power production does not necessarily follow the flow rate into the reservoir, the stabilization of the upstream water level $h_U(t)$ becomes a central challenge. The latter is defined by the differential equation

$$\dot{h}_U(t) = \frac{Q(t) - Q_B(t)}{A_{res}} - \frac{P_{B,i} + P_C(t)}{(h_U(t) - h_D(t))} \cdot \frac{1}{A_{res} \cdot \rho \cdot g \cdot \eta} \tag{1}$$

with

$Q_B(t)$ bypass water
$\rho = 1000 \frac{kg}{m^3}$ density of water
$g = 9.81 \frac{m}{s^2}$ gravitational constant.

When interpreting the hydro-plant as a dynamic control system, the three time variable values

- balancing power $P_C(t)$
- discharge into the reservoir $Q(t)$
- downstream water level $h_D(t)$

have the function of disturbance inputs impeding the stabilization of the upstream water level. The produced balancing energy $P_C(t)$ and the discharge $Q(t)$ were fed into the simulation as 15-minute-values. The downstream water levels $h_D(t)$, however, were available only in a daily

resolution.

The bypass water $Q_B(t)$ is composed of the water spilled over the weir, when exceeding the capacity of the reservoir and the residual flow rate through other bypass streams e.g. fish ladders. Since the latter are neglected in this model $Q_B(t) = 0$ when the reservoir is not completely filled.

$$Q_B = \begin{cases} Q(t) - Q_P & for\ h_U(t) \geq h_U^{max} \wedge Q(t) > Q_P \\ 0 & else \end{cases} \quad (2)$$

with

Q_P flow rate through the plant
h_U^{max} maximum upstream water level

In equation (1) the available head $H(t) = h_U(t) - h_D(t)$ appears as a denominator in the second term. As a result, the influence of the disturbance inputs $P_C(t)$ and $h_D(t)$ considerably increases, the lower the (nominal) head gets. From this perspective the simulated low-head plant in Bannetze-Hornbostel can be considered as a conservative scenario.

In the theoretical case of an undisturbed control system $P_C(t)$, $Q(t)$ and $h_D(t)$ can be considered time-constant. As a result, for $h_U(t) < h_U^{max}$ the second derivative of the upstream reservoir level during a delivery interval of constant base power i is defined as

$$\ddot{h}_U(t) = \dot{h}_U(t) \cdot \frac{P_{B,i} + P_C}{(h_U(t) - h_D)^2} \cdot \frac{1}{A_{res} \cdot \rho \cdot g \cdot \eta}. \quad (3)$$

Since the two right factors $\frac{P_{B,i}+P_C}{(h_U(t)-h_D)^2}$ and $\frac{1}{A_{res}\cdot\rho\cdot g\cdot\eta}$ can never become negative, the condition

$$sgn\left(\ddot{h}_U\right) = sgn\left(\dot{h}_U\right) \quad (4)$$

is always fulfilled. As a consequence, an initial increase/decrease of the upstream water level will keep growing/falling at an ever increasing speed. This means, that the upstream reservoir level $h_U(t)$ behaves unstable. As soon as the maximum upstream water level h_U^{max} is reached the excessive water has to be spilled over the weirs. When reaching the minimum water level h_U^{min}, however, the plant's output power has to be reduced in order to prevent the reservoir level from falling any further. This means that the scheduled power cannot be completely produced.

Due to this behavior, a governor is necessary to stabilize the reservoir level. Together, the governor and the plant model form a closed control loop, as shown in Fig. 3. Next to the stabilization of the upstream water level the governor has the task to estimate the maximum available balancing reserve $P_{Cj,plant}^{max}$ for every coming tendering round j from current parameters. This means that the governor is responsible for the entire organization of the combined plant operation. Due to the imperfect foresight modelling approach, the governor can only estimate the future values for the disturbance inputs based on present or past data. The accuracy of these forecasts and the ability to compensate forecasting errors are therefore crucial for the balancing operation.

The upstream water level is stabilized by adjusting the base power $P_{B,i}$ after each delivery interval i. Here, the governor makes use of the fact that higher power outputs lead to an increased water intake and thus reduce the gradients of the upstream water level and vice versa (see equation (1)). The governor's setting frequency is therefore determined by the duration of each delivery interval t_D. Since contracts on the energy only markets are usually traded with a certain lead time t_L before the start of delivery, there is an additional delay between the determination of the future base power and its start of delivery. Consequently, the time span between the calculation of the correcting variable $P_{B,i}$ and its effect on the system ranges between

$$t_L \leq \Delta t \leq t_L + t_D. \quad (5)$$

Both, too long delivery times t_D and lead times t_L therefore complicate the stabilization of the upstream water level.

The required base power $P_{B,i}$ is calculated in two consecutive steps at t_0, as shown in Fig. 4. In the first step, the governor estimates the upstream water level $h_U(t_1)$ at the start of the next delivery interval that will be theoretically reached with the current system parameters such as base power and discharge to the reservoir (blue line). In the second step, the governor calculates the future output power necessary to bring this upstream water level back to the lead value h_U^{target} by the end of that delivery interval at t_2 (red line).

For the governor's second task, the determination of the maximum marketed balancing reserves $P_{Cj,plant}^{max}$, the tender modalities play an important role. Even though older input data were used, all the simulations were conducted for the auction design valid in October 2020 in order to achieve most relevant results unless explicitly stated otherwise. An overview of these modalities is shown in Table 1.

From November 2020 on, a new market design for aFRR and mFRR was introduced with separate markets for balancing power and energy. In this design the simulation results achieved with the rules of October 2020 represent a regular bidding at gate closure of the balancing power market with no posterior adaption of the power prices. Therefore they are still up-to-date under these constraints. For results under anterior auction designs with weekly tenders for FCR and a decreased lead time for aFRR see [36].

In analogy to the base power, the calculation process itself has to be executed latest at the gate closure time of each coming tendering interval. This is between 14 and 16 h before the start of delivery, depending on the balancing service.

In order to eradicate the influence of the bidding strategy, the activation of balancing energy in the merit order of the lowest price offers was neglected in the simulations. Instead it was assumed that all available capacities are simultaneously activated according to their total

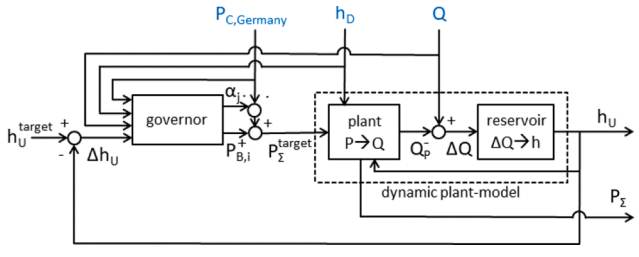


Fig. 3. Block diagram of the control loop.

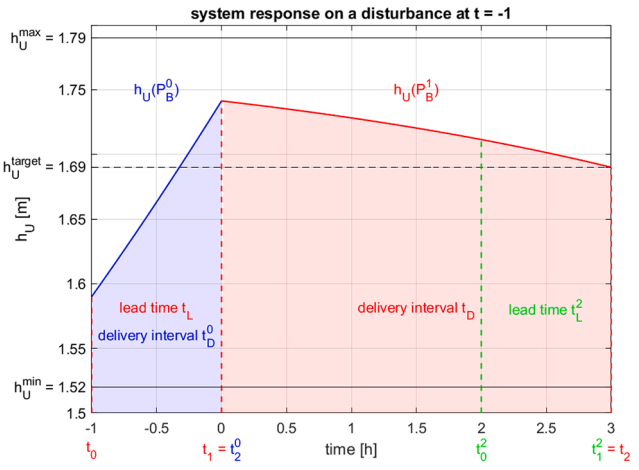


Fig. 4. Step response of the undisturbed system with an exemplary lead value of $h_U^{target} = 1.69$ m to an initial upstream water level of $h_U(t_0) = 1.59$ m and an insufficient initial base power production.

Table 1
tender modalities of balancing services used in the simulation.

tender modalities for balancing services	balancing service		
	FCR	*aFRR*	*mFRR*
delivery time	daily 24 h	daily 24 h	daily 24 h
bidding deadline	8:00	9:00	10:00
start of delivery	next day 0:00	next day 0:00	next day 0:00
lead time	16 h	15 h	14 h

power band reserved for balancing power generation. This means that during each tendering period j, the simulated ROR-plant is targeted to deliver the same constant share $\alpha_{j,target}$ of the total balancing power activated on national level $P_{C,Germany}(t)$. This proportion also corresponds to the ratio of the balancing capacity awarded in the auction $P^{max}_{Cj,plant}$ to the total amount of balancing power announced in the tender $P^{max}_{Cj,Germany}$:

$$\alpha_{j,target} = \frac{P_{C,target}(t)}{P_{C,Germany}(t)} = \frac{P^{max}_{Cj,plant}}{P^{max}_{Cj,Germany}}. \tag{6}$$

Consequently, the target balancing power demanded from the plant is

$$P_{C,target}(t) = \begin{cases} \alpha^{+}_{j,target} \cdot P_{C,Germany}(t) & for P_{C,Germany} > 0 \\ \alpha^{-}_{j,target} \cdot P_{C,Germany}(t) & else \end{cases} \tag{7}$$

The governor can manipulate the amount of marketed automatic and manual frequency restoration reserve by adjusting the target delivery factors $\alpha^{+}_{j,target}$ and $\alpha^{-}_{j,target}$. These factors are calculated based on the plant's positive and negative power reserves. In the current model these power reserves are forecast based on current system parameters and a hydrodynamic model. However, since no weather forecasts are taken into account the prediction accuracy is rather limited. In order to manage the inevitable risk of forecast errors the estimated positive and negative power reserves are additionally multiplied by freely selectable marketing factors $0 \leq \kappa^{+} \leq 1.5$ and $0 \leq \kappa^{-} \leq 1.5$.

$$\begin{aligned} \alpha^{+}_{j,target} &= \kappa^{+} \cdot \frac{P^{+}_{res,j}}{P^{max+}_{Cj,Germany}} \\ \alpha^{-}_{j,target} &= \kappa^{-} \cdot \frac{P^{-}_{res,j}}{P^{max-}_{Cj,Germany}} \end{aligned} \tag{8}$$

with

$P^{+}_{res,j}$, $P^{-}_{res,j}$ minimum forecast positive and negative power reserves during coming delivery interval j

Hence, this pair of marketing factors $\kappa_ = (\kappa^{+}; \kappa^{-})$ determines the share of the predicted power reserves that will be offered as balancing capacity in the upcoming auction. When κ^{+} or $\kappa^{-}$are equal to zero, neither positive nor negative balancing service are delivered. In change, at $\kappa > 1$ the marketed balancing reserve is even higher than the forecast power reserve. Consequently, the marketing factor enables a free adjustment between the amount and reliability of delivered balancing energy. It also allows to investigate the interaction between positive and negative frequency restoration reserve.

In case of FCR the positive and negative power components are marketed together in a symmetrical band. As a result, a common target delivery factor $\alpha_{j,target} = \alpha^{+}_{j,target} = \alpha^{-}_{j,target}$ is used. It is calculated from the minimum of the predicted power reserves in positive and negative direction multiplied by the common marketing factor $\kappa_ = \kappa$.

$$\alpha_{j,target} = \kappa \cdot \frac{\min\left(P^{+}_{res,j}, P^{-}_{res,j}\right)}{P^{max}_{Cj,Germany}} \tag{9}$$

Due to the risk of prediction errors for the available power reserves, a higher marketed balancing capacity (i.e. high values of κ) almost necessarily reduces the reliability of the promised deliveries. Therefore, the potentials can only be expressed as a combination of the amount and reliability of balancing energy produced. The average reliability over a considered period of time can be defined as the quotient

$$R\left(\underline{\kappa}\right) = \frac{W\left(\underline{\kappa}\right)}{W_{target}\left(\underline{\kappa}\right)} \tag{10}$$

This equals the energy actually produced over the targeted energy production. The reliability factor can be applied to the base power (R_B) as well as the different types of balancing energy (R_C for FCR and R^{+}_{C} and R^{-}_{C} for aFRR and mFRR).

For an easier interpretation, the delivered balancing energy is expressed as an extrapolated delivery factor α instead of just giving the annual work W_C:

$$\alpha\left(\underline{\kappa}\right) = \frac{W_C\left(\underline{\kappa}\right)}{W_{C,Germany}} \cdot \frac{P_{Germany}}{P_{max}} \tag{11}$$

with

$W_{C,Germany}$ national demand for balancing energy
$P_{Germany}$ national ROR-capacity.

This theoretical value is equivalent to the average share of the German balancing energy demand that can be covered by conventional ROR, when upscaling the potentials of the simulated plant in Bannetze-Hornbostel. It should not be confused with the governor's target delivery factor $a_{j,target}$ during one tendering interval j, which is not considered further when looking at the potentials. In most cases, the delivery factor α and the reliability R refer to the entire delivery period considered (i.e. 1 or 3 years). Therefore, it is important to mention that these mean values are sometimes exceeded and sometimes fallen short of.

For an economic assessment the production of both, the balancing energy W^{+}_{C} and W^{-}_{C} as well as the base energy W_B have to be considered. Next to that, the total energy production W_Σ is important to judge the ecologic performance. These values are connected via the equation

$$W_\Sigma = W_B + W^{+}_{C} + W^{-}_{C}. \tag{12}$$

The overall energy production W_Σ in balancing power mode is generally lower than the harvest during conventional operation W_{conv}. This is due to two reasons:

- additional water losses over the weir
- reduced available head due to lower average upstream water levels

The second effect is particularly strong in plants with a low head as the modelled unit in Bannetze. For an easier comparison the energy harvests can be related to the energy produced during conventional operation W_{conv}:

$$\omega_X = \frac{W_X}{W_{conv}} \quad for\ X = \{\Sigma; B; C^{+}; C^{-}\} \tag{13}$$

4. Balancing potentials of the Bannetze-Hornbostel plant

The developed deterministic simulation model was used to calculate the balancing potentials for a projected hydroelectric plant in Bannetze-Hornbostel on the Aller-river in northern Germany. The plant was modelled using the parameters in Table 2. It will be the prototype of a high-performance waterwheel technology developed at TU Braunschweig, reaching a rated power of 700 kW (see Fig. 5). The waterwheel is specially designed to yield high efficiencies at very low heads. With a

Table 2
parameters used for modelling the hydroelectric plant in Bannetze-Hornbostel

simulation parameters		
parameter	***symbol***	***value***
maximum power output	P_{max}	700 kW
maximum flow rate	Q_{max}	60 $\frac{m^3}{s}$
efficiency (constant)	η	85%
reservoir area	A_{res}	432,000 m
max. upstream water level	h_U^{max}	$h_U^{target} + 0.02\ m$
min. upstream water level	h_U^{min}	$h_U^{target} - 0.25\ m$
mean head 2015–2017 at h_U^{max}	H_{nom}	1.79 m
minimum head	H_{min}	0.30 m

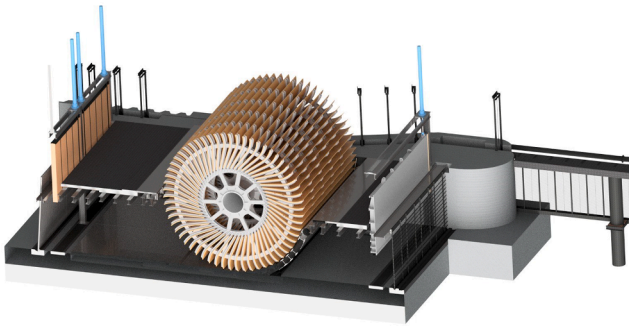


Fig. 5. Longitudinal section of the modelled research power plant with the high-performance waterwheel.

mean head of only 1.79 m and a maximum flow rate of 60 $\frac{m^3}{s}$ it will fill the technological gap at very low heads and moderate flow rates. Moreover, the plant is projected to generate electricity down to a minimum head of 30 cm. After completing the foundation the construction works on the plant were preliminarily stopped and will be taken up again in near future.

For the upstream water level a peak-to-peak amplitude of 27 cm was applied. This value corresponds to the current lead operation levels of the existing weir during summer and winter, serving as upper and lower limits. As a result, it can be assumed that a flexible upstream water level regime within these limitation will have no negative impacts. Under these conditions, a storage volume of 116,600 m^3 is achieved. This means that the empty reservoir can retain the average flow of approximately 41 $\frac{m^3}{s}$ for 47 min, before having to lead water to the downstream. At nominal downstream water levels this corresponds to a storage capacity of 405 kWh. Even though the affected part of the Aller is classified as a minor waterway, professional shipping only plays a subordinate role. Therefore it is very likely that even higher reservoir amplitudes and thus larger storage capacities could be realized. Consequently, the simulation results can be considered rather conservative.

An analysis on lead values for the upstream water level h_U^{target} within the usable bandwidth in [38] showed that maximum lead values also lead to maximum balancing service potentials despite an increasing risk of water losses over the weir. This is due to two reasons: Firstly, in case of the plant in Bannetze the increased average head overcompensates the higher weir losses and thus leads to higher overall energy yields. Secondly, more stored water is available for the production of positive balancing services which turned out to be more difficult to provide at high reliabilities. Consequently, for the simulations in this paper the lead value $h_U^{target} = h_U^{max} - 2\ cm$ only two centimeters below the upper limit was chosen.

For the base power marketing a lead time of $t_L = 1\ h$ with a time of constant delivery of $t_D = 3\ h$ was used. As shown in [38] this timeframe allows a good trade-off between the stability of the reservoir water level and the demands of the energy markets for plannable power production.

The balancing potentials of the Bannetze-Hornbostel plant were assessed by means of parameter studies over κ_-. Therefore each entry of κ_- was augmented in steps of 0.05 between 0 and 1.5 and a simulation run was conducted. This lead to parameter fields of the extrapolated achievable coverages of the national demand $\alpha(\kappa_-)$ and the corresponding reliabilities $R(\kappa_-)$. Out of these fields, representative pairs $(\alpha; R)$ of those two parameters were chosen to quantify the balancing potentials. Since there is little dependency of the marketing factor of one product (e.g. κ^+) on the values for the opposite product (e.g.$(\alpha^-; R^-)$) [38] the following method could be applied to identify the potentials from the parameter fields:

- Whenever an extrapolated full coverage of the national demand α can be achieved at a corresponding marketing factor $\kappa \leq 1.5$, the potentials are determined by the reliability at this $\alpha = 100\%$ extrapolated coverage.
- If the maximum extrapolated coverage of the national demand at a corresponding marketing factor $\kappa \leq 1.5$ is less than 100%, the potentials are determined by the achieved extrapolated coverage α at a reliability of $R = 95\%$.

$$(\alpha; R) = \begin{cases} (100\%; R(\alpha = 100\%)) & for\ \alpha(1.5) \geq 100\% \\ (\alpha(R = 95\%); 95\%) & else \end{cases} \tag{14}$$

The average achievable delivery factor $\alpha(\kappa)$ and corresponding reliability $R(\kappa)$ for FCR over the common marketing factor κ are shown in Fig. 6 for the years 2015–2017. The dashed lines break the reliability further down to the positive and the negative power component. An average extrapolated three-year coverage of more than 150% of the national demand can be reached with a mean reliability of almost 99.50%. This means that only one out of 200 kWh is not properly delivered when activated. Despite its niche role in the German electricity sector non-'peaking' ROR could therefore play an important role in future grid balancing.

For the extrapolated delivery factor no significant differences between the two power components and the mean value can be observed. The reliability, however, is generally higher for the negative power component than for the positive. Therefore, the reduction of the reliability R due to higher coverages α is especially striking for the positive power component. In order to cover an average of 100% of the national demand for both power components, a marketing factor of $\kappa = 0,87$ is

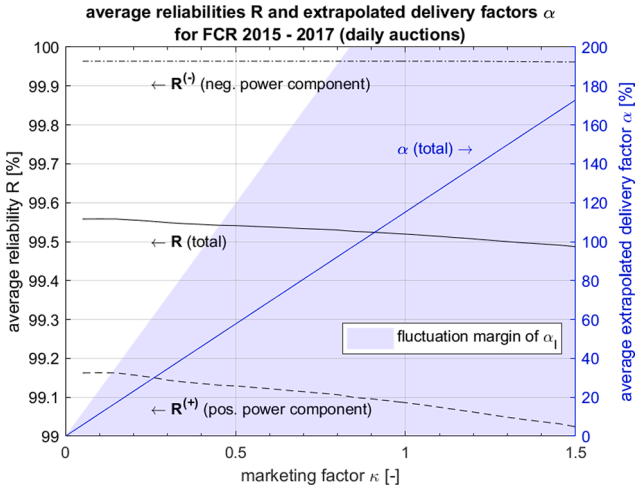


Fig. 6. Average reliability $R(\kappa)$ and achievable extrapolated shares of the national demand $\alpha(\kappa)$of frequency containment reserve over the marketing factor κ during the years 2015–2017. The reliability is further broken down to the positive and negative component of the FCR-demand. The blue area shows the spread of $\alpha_j(\kappa)$ during the different one-week delivery intervals.

necessary. This leads to an overall reliability of 99.53%.

These high average values, however, vary widely in the course of the three years considered. This is due to seasonal and climatic influences. The blue highlighting in Fig. 6 marks the range of the delivery factors $\alpha_j(\kappa)$ achieved during the 1-day tendering intervals. It indicates that the average value is sometimes exceeded by factor 2 while at other times (e.g. during flooding) no FCR can be provided at all. Since hydropower plants in the same regions underlie similar weather conditions, only relying in ROR for grid balancing bears a considerable concentration risk. This should be mitigated by supplementary technologies, such as demand side management or batteries.

In case of automatic and manual frequency restoration reserve the positive and negative balancing energy are marketed and delivered independently. This leads to an additional degree of freedom reflected by the two independent marketing factor components κ^+ and κ^-. Fig. 7 shows the achievable reliabilities and delivery factors for the positive and negative, automatic and manual frequency restoration reserve as two-dimensional parameter fields over κ^+ and κ^-. The achieved reliabilities $R^+(\kappa^+;\kappa^-)$ and $R^-(\kappa^+;\kappa^-)$ are shown as color plots with solid isolines whereas the corresponding delivery factors $\alpha^+(\kappa^+;\kappa^-)$ and $\alpha^-(\kappa^+;\kappa^-)$ are printed as dashed isolines.

Both graphs for aFRR show a high similarity with those for mFRR despite the fact that the total activated energies for aFRR are between 7 (pos. balancing) and 10 (neg. balancing) times higher than for mFRR. However, for both, manual and automatic frequency restoration reserve the negative balancing potentials are significantly higher than the positive. In the three year average the national demand for negative aFRR can be fully covered with a high reliability R^- of around 99.8%. This value reaches 98.3% for an extrapolated full coverage in case of mFRR.

The differences between the achievable extrapolated shares of the national demand $a^+$and the corresponding reliabilities R^+ of the positive frequency restoration reserve and its negative counterpart have various reasons. Firstly, in the considered years the demand for positive balancing energy was generally higher than for negative. In case of mFRR the amount of positive balancing energy activated was around 2.3-times as high as its negative equivalent. The activation of positive automatic frequency restauration reserve was approximately 40% higher than for negative aFRR. Secondly, the production of positive balancing services is affected by system throttling occurring when the upstream water level reaches the lower limit. At the same time, the plant's additional power output due to positive balancing power further increases this risk by dropping the upstream water level. Lastly, in order to keep the investment costs low, most ROR hydroelectric plants have very limited reserves in terms of net power output and maximum flow rate. This narrows the available band for providing positive balancing power especially at times of high natural discharge.

Since a full extrapolated coverage of the national demand at $\kappa^+ \leq 1.5$ is not possible for neither type of positive frequency restoration reserve, a minimum average reliability of 95% is used to express the potentials.

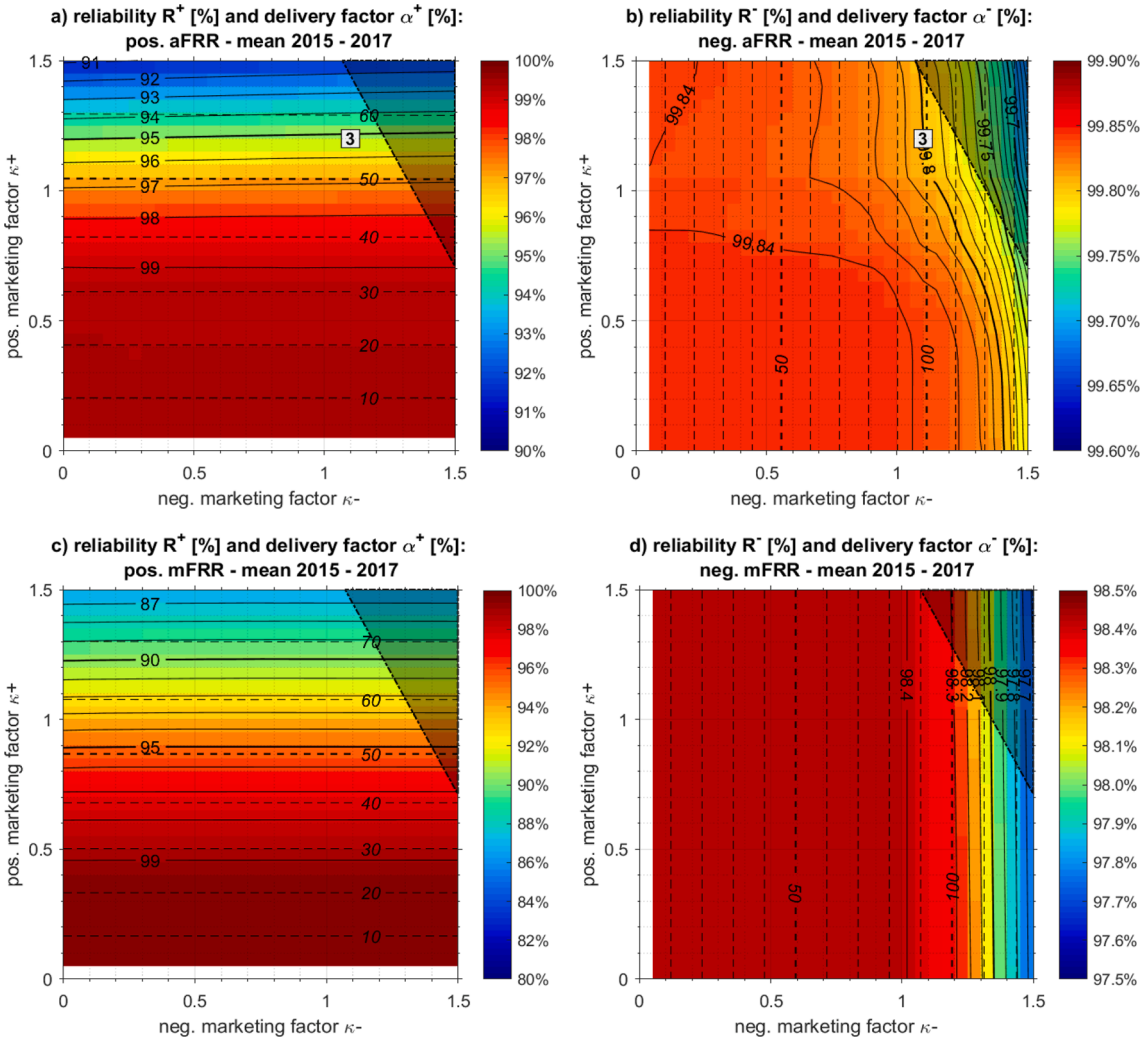


Fig. 7. Average achieved reliabilities $R(\kappa^+;\kappa^-)$(color plot and solid isolines) and corresponding extrapolated shares of national demand $\alpha(\kappa^+;\kappa^-)$ (dashed isolines) for the automatic frequency restoration reserve (top) and manual frequency restoration reserve (bottom) in the years 2015–2017.

In this case 56% of the national demand of positive aFRR and 51% of the national demand of positive mFRR can theoretically be covered by the non-'peaking' ROR-hydropower in Germany. The graphs show that a reasonable increase of reliability can only be achieved when significantly decreasing the offered balancing capacity. Consequently, backup technologies are necessary at least for the positive balancing services.

For producing these high amounts of balancing energy a notable share of the plant's maximum power output has to be reserved for balancing. In case of the described scenario for aFRR 410 kW have to be reserved for negative balancing while 240 kW have to be reserved for positive balancing, respectively. This means that the base power production is theoretically limited to the remaining band between 410 kW and 460 kW, if no further limitations (e.g. due to reaching the maximum plant flow rate) apply. For the mFRR power reserves lead to a theoretical base power band between 440 kW and 520 kW.

In the 15-minute values used for the simulations, however, it is very rare that the full amount of reserved balancing power is actually activated by the TSOs. Consequently, reasonable balancing energy reliabilities can still be achieved when the base power exceeds this range in any direction. Nevertheless, the sum of the power reserves offered as positive and negative balancing capacity may not exceed the maximum plant output of 700 kW, since a full delivery of the tendered power would become a priori impossible. In Fig. 7, these 'forbidden' states of too high marketing factors are marked with a dash-dotted frame and a shadow.

The reliability of the simultaneously produced base power is higher than 99.8% for all scenarios, all types of balancing services during every year considered.

In 2017 the total installed ROR-hydropower capacity accounted for only 3% of the overall electricity production in Germany [48]. In this light the potentials for all types of balancing services can be considered quite remarkable. When accepting larger amplitudes for the upstream water level and thus augmenting the storage capacity even higher reliabilities could be achieved for FCR and positive aFRR or mFRR. Consequently, ROR-hydropower can be an important stabilizer of a future energy system far beyond its current niche-role as an electricity producer. However, it is very likely that the current capacities alone will not be able to satisfy the increasing future demand for all three types of balancing power at the same time. Other technologies and/or an increase of installed ROR-capacities will therefore remain required.

5. Influence of the auction design

In July of 2018 the auctions of aFRR were changed from weekly to daily. One year later the same measure was taken for FCR. One motivation for this change was to facilitate the participation of renewable energies in the balancing markets. Fig. 8 shows the mean FCR-potentials in the years 2015–2017 for different auction designs. Unlike the previous graphs the potentials are given as relative delivery failures defined as

$$\frac{W_{target} - W}{W_{target}} = 1 - R. \tag{15}$$

They are presented on a logarithmic scale over the achieved extrapolated ROR-coverage α during these years. The red line represents the weekly auctions before 2019 with a lead time of 129 h (bidding time: Tuesday by 15:00) and a delivery time of 169 h (one week). The blue line shows the current daily auction design with a lead time of 16 h and a delivery time of 24 h. Next to that, the green line expresses a hypothetic case were the auctions take place twice a day with a bidding deadline 8 h before the start of delivery.

As the graph shows, the implementation of daily auctions reduced the delivery failures by roughly one order of magnitude. This means, for example, that the reliability for an extrapolated full coverage of the national demand was increased from 95.0% to 99.5%. Such an increase would have a huge impact on the requirement for backup capacities. In

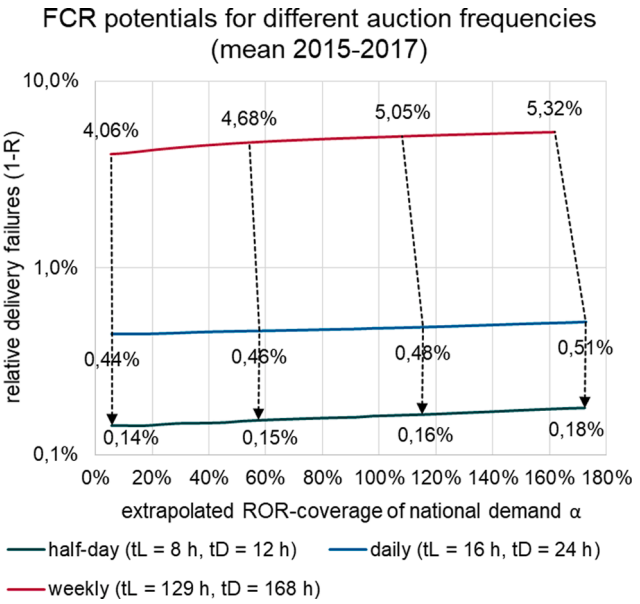


Fig. 8. Relative delivery failures of frequency containment reserve over the achieved extrapolated coverage of the national demand for different auction intervals on a logarithmic scale in the years 2015–2017.

case of auctions twice a day, the reliability increases even further to 99.8%. Consequently, halving the lead and delivery time would further decrease the delivery failures by approximately factor 3. The reason for these higher potentials is that the governor can react a lot faster to changing environmental conditions, such as altering flow rates to the reservoir or downstream water levels. This allows a quicker reduction of the offered power reserves in case these conditions worsen (e.g. when the plant is switched off due to flooding) and thus decreases the amount of delivery failures.

The dashed arrows in the graph mark points of equal marketing factors κ, namely $\kappa = \{0.05; 0.5; 1.0; 1.5\}$ from left to right. As the arrows reveal the potentials are not only increased by higher reliabilities (i.e. lower relative delivery failures), but also by higher amounts of energy actually delivered (α). Since the amounts of marketed FCR hardly differ for the three considered auction designs, this increase in α can, again, be highly related to the decrease of the delivery failures $1 - R$.

Reducing the auctions from weekly to daily shows a similar effect on aFRR. Daily auctions allow the delivery of 56% of positive aFRR with a reliability of 95%. For the same coverage a reliability of only 88% was reached in the previous weekly auction design. When demanding a minimum reliability of 95%, as little as 5% of the demand for positive aFRR can be theoretically be covered. A full coverage of the demand for negative aFRR is still possible under weekly auctions, yet the reliability significantly reduces to 98.4%.

For aFRR and mFRR the introduction of separate markets for balancing power and energy introduced in November 2020 allows the placement of balancing energy bids also for actors who were not successful on the power auctions. In this case the gate closure time is only one hour before the start of delivery. With a delivery time of only 4 h, further increases of the ROR-potentials can be expected. For these free bids, however, no power price is granted.

It can be summarized, that the reduction of auction intervals significantly increased the balancing energy potentials of ROR-hydropower. Similar effects can be expected for other renewable energy sources. Therefore these changes in the market design can be considered a successful step for opening the balancing service markets to renewable energies and a low hanging fruit for increasing the potentials of ROR-hydropower.

6. Revenues and impacts on greenhouse gas emissions

The production of balancing energy leads to a lower overall energy production and has an influence on the remaining base energy that can be sold on the energy only markets. Therefore the relative power productions ω_Σ and ω_B compared to conventional operation are conclusive indicators for the economic potentials and impacts of balancing operation.

The corresponding underproductions $1-\omega_\Sigma$ and $1-\omega_B$ when providing aFRR are shown in Fig. 9 as a parameter field over $\kappa_- = (\kappa^+;\kappa^-)$. The red line marks points where the sum $W_C^+ + W_C^- = 0$ and thus the total energy production is equal to the base energy produced ($W_\Sigma = W_B$).

In the years 2015–2017 the relative underproduction of total energy $1-\omega_\Sigma$ ranges between 1.4% and 8.0%, depending on the marketing factors chosen. The lowest gradients of the total underproduction all occur at $\kappa^- = 0$, pointing in the direction of κ^+. Hence, for all positive marketing factors the maximum energy production is realized when no negative balancing service is produced. This is because the total energy losses are dominated by the additional weir losses, which can sum to more than 6.3% at $\kappa_- = (0;1.50)$. They behave approximately proportional to the amount of negative balancing energy produced and thus are close to zero at $\kappa^- = 0$.

The influence of the head losses on the total underproduction $1-\omega_\Sigma$ is significantly lower. They reach their maximum of 3.5% at $\kappa_- = (1.50;0)$ and increase, the higher the amount of positive balancing energy gets. In a smaller extent the head-losses also grow with a decreasing amount of negative balancing energy. In Fig. 9, this loss mechanism can be identified as the growing total underproduction $1-\omega_\Sigma$, when increasing κ^+ at constant negative marketing factors κ^- (i.e. moving vertically upwards in the graph). These sum of these two loss mechanisms are the reason, why the maximum total energy losses $1-\omega_\Sigma$ occur at the point of the highest balancing power production at $\kappa_- = (1.5;1.5)$.

The economic viability will be discussed on four different production scenarios. As it depends on the amounts and prices of the energy products, the relative production of base energy ω_B and the balancing services have to be considered, rather than ω_Σ. While for FCR only a power price is granted, aFRR and generate mFRR revenues from the total capacity reserved (power price) and from the amount of balancing energy actually delivered (energy price). Due to the pay-as-bid remuneration these revenues strongly depend on the bidding strategy. In order to eradicate this factor of uncertainty, national average prices for the reserved balancing capacities and the activated balancing energy were used. The base power only receives an energy price which can be a fixed feed-in tariff or the fluctuating prices on the electricity markets. For the latter, German wholesale market prices of the corresponding years were used. Although the energy prices of both, base power and negative frequency restoration reserve can eventually become negative, their average prices remained positive in the years 2015–2017 [49].

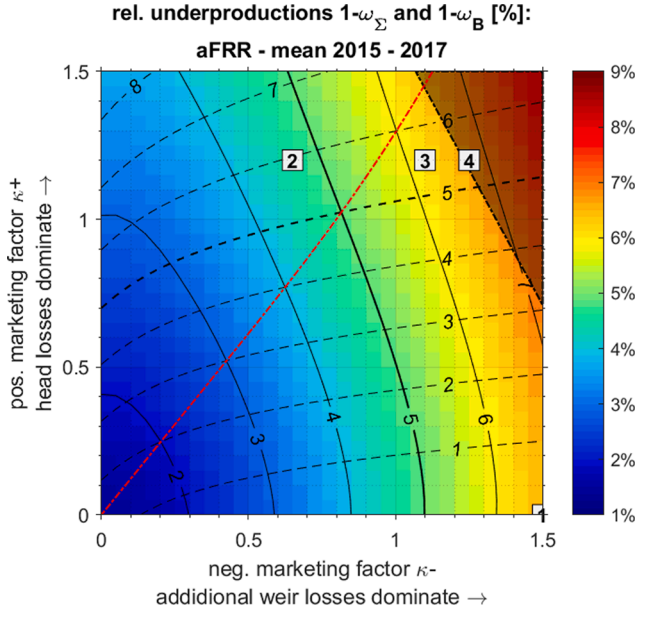


Fig. 9. Average total underproduction $1-\omega_\Sigma$ (color plot and solid isolines) and underproduction of base power $1-\omega_B$ (dash-dotted isolines) in relation to the conventional energy production for the production of automatic frequency restoration reserve in the years 2015–2017.

The energy balance in equation (12) indicates that the base power production W_B is getting higher than the total energy production W_Σ for $-W_C^- > W_C^+$. In Fig. 9 this applies to the area on the right side of the red line. An extreme case is marked as scenario 1 at $\kappa_- = (0;1.5)$ on the right bottom of the figure. It represents the maximum (simulated) production of negative aFRR and no production of its positive counterpart at all. Here, the great imbalance $-W_C^- \gg W_C^+$ even outweighs the total underproduction $1-\omega_\Sigma$ so that the base energy production remains the same as in conventional operation. The negative balancing energy produced sums up to 6.6% of the conventional energy harvest with a corresponding power price granted for 79.7% of the net output power, equivalent to 560 kW. When assuming that the same (time-variable) base-power prices are achieved during conventional and balancing operation and average prices for all products are positive, providing balancing services therefore securely leads to additional revenues. When marketing the base power on the wholesale markets the additional incomes sum up to 3.6%. The relative energy productions ω and revenue surplus compared to conventional operation ψ of this and other highlighted scenarios are listed in Table 3. .

The additional incomes ψ during balancing operation are also shown in Fig. 10. Here, it can be observed that delivering positive balancing services is a lot more attractive than their negative counterpart, even though less base energy can be sold alongside. This is due to far higher prices achieved for positive balancing services. During the years considered the energy prices, for example, were about 20-times as high as for negative balancing energy and amounted around 1.6-times the base energy prices.

However, the total underproduction resulting from balancing operation has to be compensated by - mainly fossil - residual capacities. Data published in [50–52] lead to an emission factor of the non-renewable net energy production for 2019 of 682 $\frac{g}{kWh}$. Consequently, the lost overall production of green energy in scenario 1 would indirectly lead to annual CO_2-emissions of 173 t per year in the remaining generation park. This means that for each 1000 € of additional income for the plant an extra 62 t of CO_2 are emitted by the remaining generation pool. These 'opportunity emissions' are particularly high for the plant in Bannetze, as

Table 3
mean energy production 2015–2017 of total energy, base power and balancing energy as relative shares of the energy harvest in conventional operation for different automatic frequency restoration reserve scenarios

energy balance and revenues for the delivery of aFRR 2015-2017						
scenario number		#	1	2	3	4
marketing factor	positive	κ^+	0	1.20	1.20	1.20
	negative	κ^-	1.50	0.65	1.10	1.25
rel. energy production	total energy	ω_Σ	93.3%	95.3%	93.8%	93.2%
	base power	ω_B	100%	94.1%	94.5%	94.6%
	pos. aFRR	ω_C^+	0%	4.1%	4.1%	4.1%
	neg. aFRR	ω_C^-	−6.6%	−2.9%	−4.9%	−5.5%
additional revenue		ψ	3.6%	11.2%	12.7%	13.2%

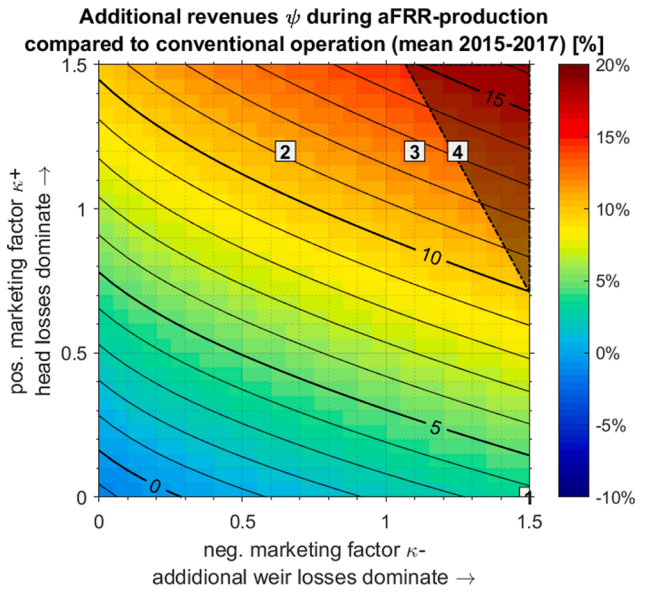


Fig. 10. Additional revenues ψ during the production of automatic frequency restoration reserve compared to conventional operation in the years 2015–2017.

its low head leads to notably higher underproductions due to reduced upstream water levels. Therefore, at a current situation with no significant lack of capacities, a balancing power operation as outlined in this paper should be considered carefully from an ecological point of view.

Nevertheless, these 'opportunity emissions' have to be interpreted cautiously: On one hand side, they will decrease with further success to decarbonize the electricity system and finally become zero. On the other hand side, in a future energy system renewable balancing services will be a key for the further installation of fluctuating renewables. The simulated 700 kW plant alone is able to provide a symmetric band of ±240 kW of aFRR at a minimum reliability of 95% (scenario 2). According to [9], this enables the installation of 3.4 MW to 8.1 MW of wind power or PV that drive residual production out of the grid. With average full load hours of 1900 $\frac{h}{a}$ for onshore wind and 970 $\frac{h}{a}$ for PV, the balancing power production would thus lead to emission savings of 2300 $\frac{t_{CO_2}}{a}$ to 10,500 $\frac{t_{CO_2}}{a}$ [51]. This is between 19 and 86-times the 'opportunity emissions' caused by producing this symmetric band.

As stated above, an extrapolation of these figures to national level comes along with high uncertainties, as the potentials vastly differ among the different ROR-units. However, it is a useful way to illustrate the scale of the simulated plant's potentials. Extrapolated on national level ROR-hydropower would indirectly be responsible for additional emissions of 540,000 t_{CO_2} per year in scenario 2. At the same time, this enables between 15 GW and 36 GW of additional fluctuating renewables, saving between 10 Mt and 47 Mt of emissions. According to these extrapolations, using ROR for balancing services could theoretically help increasing the capacities of installed onshore wind and PV by 25–59%. This would reduce the emissions of the national energy sector by 5–21%.

To summarize, grid balancing by ROR-hydropower leads to increased emissions in the current electricity system where enough other technologies are available. However, when there is a lack of balancing capacities, ROR hydroelectric plants can play an important role as an enabler for additional renewable energies urgently needed for the decarbonization of other sectors as heat and transport.

Scenario 3 represents the case discussed in 'balancing potentials' where the negative demand for aFRR is theoretically fully covered and positive balancing energy is delivered with an average reliability of 95%. In this situation the base energy production decreases by 5.5% compared to scenario 1 and conventional operation. Nevertheless, the additional revenues (given no feed-in tariff) notably increase from 3.6% in scenario 1 to 12.7% due to the additional revenues from positive aFRR. The total energy production is 6.2% less than in conventional operation but slightly higher than in scenario 1. This would lead to 'opportunity emissions' of 162 t_{CO_2} per year in the current energy system, equivalent to 11.2 t_{CO_2} per 1000 € additionally generated by the plant. Again, this figure only applies to the current energy system without scarcity of balancing capacities and will finally reduce down to zero in a fully decarbonized energy system.

When a minimum average reliability of 95% shall be guaranteed for positive and negative aFRR, from an economic point of view it makes sense to further increase the delivery of the negative balancing service. This leads to increased revenues for both, base power and negative aFRR. An extreme case is given by scenario 4. Here the whole power output of the plant is marketed as balancing reserve, namely 240 kW for positive and 460 kW for negative aFRR. Next to a 56% coverage of the demand for positive aFRR, an extrapolated 112% of the negative demand can be covered with a reliability of 99.8%. Whereas the base power underproduction $1-\omega_B$ decreases only slightly to 5.4%, the higher share of negative balancing energy leads to a reduction of total energy produced of 6.8%. This means that 176 t_{CO_2} per year are less saved on plant level. The revenues, however, are 13.2% higher than in conventional operation. In average this means that per 1000 € of additional revenue, 11.9 tons of CO_2 would be indirectly caused.

As stated, the additional revenues ψ for the scenarios were calculated based on a remuneration of the base power at wholesale prices on the energy markets. In scenario 1 additional revenues are generated independently of the price the base power production. For the other scenarios the economic feasibility can entirely change, when plants achieve higher base power prices e.g. due to feed-in tariffs. In 2015 around 98% of German ROR-plants received a feed-in tariff. However, due to their smaller average size, these plants only accounted for one third of the electricity produced by ROR-hydropower. This suggests that there still remain high economic potentials for balancing services.

The impacts of the base power remuneration on the revenues in the different scenarios are shown in Fig. 11. At the average wholesale prices of 33 $\frac{€}{MWh}$ between 2015 and 2017 (no energy is produced at times of negative prices) scenarios 3 and 4 are a lot more attractive than scenario 1. Furthermore, scenario 4 is economically superior to scenario 3 in any case, since the merchantable base energy and further the negative balancing energy production are higher. Nevertheless, both scenarios show a far higher sensitivity to the energy only prices than scenario 1. Therefore, at energy prices higher than 102 $\frac{€}{MWh}$ for scenario 3 and 105

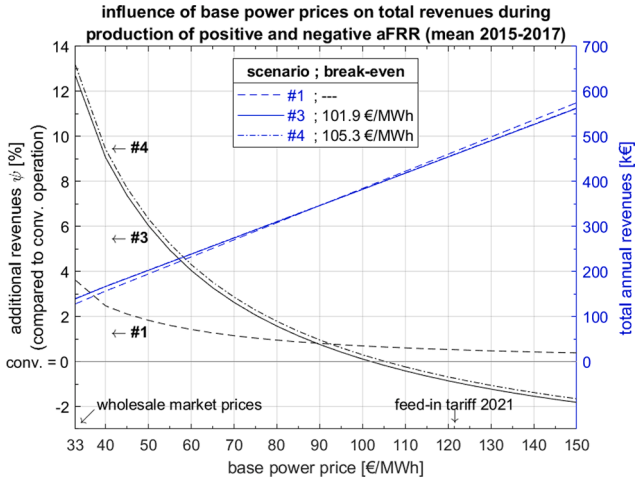


Fig. 11. Influence of the average base power prices on revenues for different production scenarios of automatic frequency restoration reserve in the years 2015–2017.

$\frac{€}{MWh}$ for scenario 4, respectively, providing balancing services is no longer economic. At this high base energy price the overall revenues have almost tripled compared to wholesale remuneration.

The modelled research power plant will presumably be remunerated by the feed-in tariff of 2021. As a result an economic feasibility of these scenarios is not given. Yet, a minor increase in revenues of 0.5% or 2400 € per year can be achieved in scenario 1, when only a maximum amount of negative balancing energy and no positive aFRR are produced.

7. Summary

Varying the upstream water level by a peak-to-peak amplitude of 30 cm is technically feasible for most ROR hydroelectric plants in Germany. From an ecologic point of view this can be desirable, as it simulates natural river dynamics with riparian areas being flooded and falling dry again. In the simulated 700 kW hydroelectric plant making use of a low amplitude of only 27 cm releases short term storage potentials of 405 kWh. This is enough to uncouple the plant's power output from the river's flow rate for a short period of time, enabling the production of balancing services next to a base power production. Unlike conventional ROR-operation, the base power can be exactly scheduled with a lead time of 1 h and held constant during a delivery time of 3 h. This schedule is complied with at a reliability of more than 99.8%, resulting in significantly reduced marketing risks.

For an easier interpretation of the simulation results, the potentials of the investigated plant in Bannetze were extrapolated to the whole German non-'hydropeaking' ROR-capacity. They are expressed as the share of the national demand for the different balancing products that could theoretically be covered. In case of FCR, this leads to a theoretical full coverage of the national demand in the years 2015–2017 with an average reliability of 99.5%. This high reliability was also achieved due to the recent change in the FCR-auctions from weekly to daily, as the average value achieved with weekly tenders was only 95.0%. Although there is a major influence of the hydrologic circumstances and the results cannot easily be applied to other sites, ROR-hydropower can be generally expected to bear high grid balancing potentials. This becomes especially clear, when taking into account that the German ROR-hydropower accounts for only 3% of the national energy mix.

In case of aFRR and mFRR, the potentials for negative balancing services are a lot higher than for positive. This is not only because the demand for negative frequency restoration reserve is lower than for its positive counterpart, but also due to higher impacts of water scarcity on the production of positive balancing services. Therefore, a full extrapolated coverage of the national demand is only possible for negative aFRR and mFRR with average reliabilities of 99.8% and 98.3%, respectively. For their positive equivalents, in contrast, a minimum reliability of 95% was chosen as a criteria for the considered scenarios. Under these conditions an extrapolated share of 56% of the national demand for positive aFRR and 51% of the demand for positive mFRR can be covered. For aFRR, it could be demonstrated that the reduction of the tendering intervals from weekly to daily in 2018 significantly increased the potentials due to lower forecasting periods.

An economic analysis for different scenarios of positive and negative aFRR-production proved that additional revenues can be generated. However, the economic feasibility strongly depends on the production scenario and the remuneration of the residual base energy harvest. When no feed-in tariff or other subsidies are granted, highest revenues can be achieved with a maximum production of both, positive and negative balancing services. In the maximum production scenario 4 where the only limitation is a minimum reliability of 95% for both balancing products, an additional 13.2% of income can be generated between 2015 and 2017. Yet, for plants receiving an average base power remuneration of 105.3 $\frac{€}{MWh}$ or more, balancing energy production is no longer feasible. This is because the base energy production is significantly lower than during conventional operation. In contrast to that, in scenario 1 where no positive but high amounts of negative balancing energy are produced additional revenues can be generated for any base power price. Here, the additional incomes range between 3.6% for wholesale market prices and 0.5% for the feed-in tariff for 2021.

Due to lower average water levels and additional water losses over the weir, providing balancing energy generally reduces the overall energy production. This effect is especially high for plants with low heads as the simulated unit. Therefore, on one hand side, balancing power operation in ROR-facilities currently induces additional emissions in the remaining fossil power stations. On plant level these 'opportunity emissions' sum up to 173 $\frac{t_{CO_2}}{a}$ for scenario 1 and 176 $\frac{t_{CO_2}}{a}$ for scenario 4. On the other hand side, ROR-balancing services are an enabler for the installation of additional fluctuating renewable energy sources as wind and photovoltaics and/or the decommissioning of fossil power plants. A 1 MW-ROR-plant offering a symmetric balancing power band at a minimum reliability 95% thus prepares the ground for 5 MW to 12 MW of new photovoltaics or wind power. When taking this into account, the reduced annual production in the ROR-plant is overcompensated between 19 and 86-times. Given the hypothetic case that all plants in Germany have similar potentials, ROR could enable an additional 25–59% of the current wind power capacities, leading to emission reductions of the national energy sector of 5% to 21%. This underlines the important role that ROR-hydropower can play in a future decarbonized energy system far beyond the production of clean energy.

CRediT authorship contribution statement

Bastian Hase: Conceptualization, Methodology, Software, Validation, Investigation, Writing - original draft, Project administration. **Christian Seidel:** Conceptualization, Validation, Resources, Writing - review & editing.

Declaration of Competing Interest

The authors declare that they have no known competing financial interests or personal relationships that could have appeared to influence the work reported in this paper.

Acknowledgment

The authors thank the foundation 'Stiftung Nagelschneider' for providing the funds for this research project. The funders had no involvement in the study design.

Resources

15-minute values for all data on balancing services were taken from [49] except FCR activation, which was calculated from grid frequency data published by European TSOs (50Hertz and RTE). Hydraulic data was provided by the federal waterway authorities. Simulations were conducted in Matlab® and Simulink®.

References

[1] BMWi. Integrierter Nationaler Energie- und Klimaplan. Bundesministerium für Wirtschaft und Energie; 2020.
[2] Deutscher Bundestag. Gesetz zur Reduzierung und zur Beendigung der Kohleverstromung und zur Änderung weiterer Gesetze (Kohleausstiegsgesetz); 2020.
[3] McKenna R. Cost-potential curves for onshore wind energy: a high-resolution analysis for Germany. Appl Energy 2014;13.
[4] Henning H-M, Palzer A. 100 % erneuerbare Energien für Strom und Wärme in Deutschland. Freiburg Im Breisgau: Fraunhofer-Institut Für Solare Energiesysteme (ISE); 2012.
[5] Agentur für erneuerbare Energien eV. Erneuerbare Energien 2020 – Potenzialatlas Deutschland. Berlin; 2010.
[6] Mainzer K. A high-resolution determination of the technical potential for residential-roof-mounted photovoltaic systems in Germany. Sol Energy 2014;17.

[7] Kunz C. Studienvergleich: Entwicklung der Volllaststunden von Kraftwerken in Deutschland; 2013.
[8] United Nations. Paris Agreement; 2015.
[9] Hirth L, Ziegenhagen I, Wind TE. Sonne und Regelleistung. Energiewirtschaftliche Tagesfragen 2013;63:2–4.
[10] dena. Studie: dena-Studie Systemdienstleistungen 2030. Deutsche Energie-Agentur GmbH (dena); 2014.
[11] Chuang AS, Schwaegerl C. Ancillary services for renewable integration. 2009 CIGRE/IEEE PES Joint Symposium Integration of Wide-Scale Renewable Resources Into the Power Delivery System, Calgary, AB, Canada: IEEE; 2009, p. 14.
[12] Holttinen H, Milligan M, Ela E, Menemenlis N, Dobschinski J, Rawn B, et al. Methodologies to determine operating reserves due to increased wind power. IEEE Trans Sustain Energy 2012;3:713–23. https://doi.org/10.1109/TSTE.2012.2208207.
[13] European Commission. Commission Regulation (EU) 2017/ 1485 - establishing a guideline on electricity transmission system operation; 2017.
[14] SAFA. Synchronous Area Framework Agreement for Regional Group Continental Europe - Annex 1: Policy on Load-Frequency Control and Reserves; 2019.
[15] Huertas-Hernando D, Farahmand H, Holttinen H, Kiviluoma J, Rinne E, Söder L, et al. Hydro power flexibility for power systems with variable renewable energy sources: an IEA Task 25 collaboration. WIREs Energy Environ 2017;6:e220. https://doi.org/10.1002/wene.220.
[16] Bayerische Wasserkraftwerke AG. Der Lech und der Lechausbau. München; 1988.
[17] Hirth L. The benefits of flexibility: the value of wind energy with hydropower. Appl Energy 2016;181:210–23. https://doi.org/10.1016/j.apenergy.2016.07.039.
[18] MVV. Regelenergie Quartalsbericht; 2016.
[19] Brucker M. Wasserkraft als Netzdienstleister am Beispiel der E.ON Wasserkraft GmbH. In: Heimerl S, editor. Wasserkraftprojekte, Wiesbaden: Springer Fachmedien Wiesbaden; 2013, p. 129–34. Doi: 10.1007/978-3-658-00996-0_17.
[20] Weiss O, Pareschi G, Schwery O, Bolla M, Georges G, Boulouchos K. Long-term scheduling model of Swiss hydropower. 2019 16th International Conference on the European Energy Market (EEM), Ljubljana, Slovenia: IEEE; 2019, p. 1–5. Doi: 10.1109/EEM.2019.8916260.
[21] Schillinger M, Weigt H, Barry M, Schumann R. Hydropower operation in a changing environment. 2017 14th International Conference on the European Energy Market (EEM), Dresden, Germany: IEEE; 2017, p. 1–6. Doi: 10.1109/EEM.2017.7981887.
[22] Yang W, Norrlund P, Saarinen L, Witt A, Smith B, Yang J, et al. Burden on hydropower units for short-term balancing of renewable power systems. Nat Commun 2018;9:2633. https://doi.org/10.1038/s41467-018-05060-4.
[23] BUWAL. Gewässerökologische Auswirkungen des Schwallbetriebs - Ergebnisse einer Literaturstudie; 2003.
[24] Meile T, Fette M, Baumann P. Synthesebericht Schwall/Sunk - Publikation des Rhone-Thur Projektes; 2005.
[25] Weiss B. Die Problematik von Schwall und Sunk in Österreich; 2010. Doi: 10.5169/SEALS-856043.
[26] Schweizer S, Tonolla D, Bruder A, Vollenweider S. Schwall und Sunk – ein kurzer Überblick 2015:6.
[27] Hunter MA. Hydropower flow fluctuations and salmonids: a review of the biological effects, mechanical causes, and options for mitigation. State of Washington, Department of Fisheries, Habitat Management Division; 1992.
[28] Heimerl S, Giesecke J. Wasserkraftanteil an der elektrischen Stromerzeugung in Deutschland 2003. Wasserwirtschaft 2004;94:28–40.
[29] Anderer P. Vorbereitung und Begleitung bei der Erstellung eines Erfahrungsberichts gemäß § 97 Erneuerbare-Energien-Gesetz - Teilvorhaben II d: Wasserkraft 2018.
[30] next Kraftwerke. Eine neue industrielle Revolution. NEXT Kraftwerke - Referenzen 2018. www.next-kraftwerke.de/unternehmen/referenzen/wasserkraft-oesterreich.
[31] Seidel C. Regelleistung und Kurzzeitspeicherung bei Laufwasserkraftwerken. VGB PowerTech J 2015:34–41.
[32] Fischer P, Stammel B, Lang P, Schwab A, Cyffka B. Hydrologische Dynamik als Motor für die Renaturierung von Auenhabitaten an der Donau zwischen Neuburg und Ingolstadt. Berichte des Lehrstuhls und der Versuchsanstalt für Wasserbau und Wasserwirtschaft, München: 2013, p. 13.
[33] Mayer Oliver, Wieprecht, Silke, Wieprecht S, Fink T. Hydroelectric power as a substitute for wind power; Wasser marsch bei Flaute. Erneuerbare Energien 2010; 20.
[34] Sundermeier, A, Schröder U, Wolters B. Zum Einfluss des Wellenschlags auf Röhricht an der Unteren Havel-Wasserstraße 2007.
[35] Rothstein B, Lerche L, Süss A-R. Möglichkeiten einer Regelenergiebereitstellung durch Laufwasserkraftwerke dargestellt am Beispiel des Unteren Neckars. Korrespondenz Wasserwirtschaft 2015:290–5.
[36] Seidel C. Mögliche Flexibilisierungspotenziale der Wasserkraft in Deutschland. Wasserwirtschaft 2017:40–4.
[37] Conrad J. Netzentlastung durch Laufwasserkraftwerke. BWK 2016:52–4.
[38] Hase B, Seidel C. Frequency control by run-of-river hydropower: A case study on energetic and economic potentials. Proceedings of GSM 2020, Lucerne: 2020. Doi: 10.5281/zenodo.4284325.
[39] Netzregelverbund. Präqualifizierte Leistung in Deutschland; 2020.
[40] Verband der Netzbetreiber. TransmissionCode 2007 - Netz- und Systemregeln der deutschen Übertragungsnetzbetreiber; 2007.
[41] Netzregelverbund. Information zum Netzregelverbund und der internationalen Weiterentwicklung (Marktinformation 04/2020); 2020.
[42] Hecker C, Zauner E, Pellinger C, Carr L, Hötzl S. Modellierung der flexiblen Energiebereitstellung von Wasserkraftwerken in Europa. Proceedings of the 9th Internationale Energiewirtschaftstagung (IEWT), Vienna, Austria 2015:11–3.
[43] Maniak U. Hydrologie und Wasserwirtschaft: Eine Einführung für Ingenieure. Berlin, Heidelberg: Springer Berlin Heidelberg; 2016. Doi: 10.1007/978-3-662-49087-7.
[44] Weisrock G. Hydropower : a vital asset in a power system with increased need for flexibility and firm capacity. Encyclopédie de l'Énergie 2016:9.
[45] Demello F, Koessler R, Agee J, Anderson P, Doudna J, Fish J, et al. Hydraulic turbine and turbine control models for system dynamic studies. IEEE Trans Power Syst 1992;7:167–79.
[46] Giosio DR, Henderson AD, Walker JM, Brandner PA. Physics based hydraulic turbine model for system dynamics studies. IEEE Trans Power Syst 2016. https://doi.org/10.1109/TPWRS.2016.2574330.
[47] Fang H, Chen L, Dlakavu N, Shen Z. Basic modeling and simulation tool for analysis of hydraulic transients in hydroelectric power plants. IEEE Trans Energy Convers 2008;23:8.
[48] ENTSO-E. Statistical Factsheet 2017; 2018.
[49] Bundesnetzagentur. SMARD Strommarktdaten n.d. www.smard.de.
[50] AGEB. Auswertungstabellen zur Energiebilanz Deutschland - Daten für die Jahre von 1990 bis 2019; 2020.
[51] BMWi. Zeitreihen zur Entwicklung der erneuerbaren Energien in Deutschland 1990 – 2019; 2020.
[52] Icha P, Kuhs G. Entwicklung der spezifischen Kohlendioxid-Emissionen des deutschen Strommix in den Jahren 1990 - 2019. Dessau-Roßlau: Umweltbundesamt; 2020.